Korea-Australia Rheology Journal
Vol. 17, No. 4, December 2005 pp. 181-190

Rheology of flocculated kaolinite dispersions

A.J. McFarlane, J. Addai-Mensah* and K. Bremmell
Ian Wark Research Institute, University of South Australia, Mawson Lakes, Adelaide S.A. 5095, Australia.
(Received August 5, 2005; final revision received November 4, 2005)

Abstract

Rheological characterisation of flocculated kaolinite pulps has been undertaken to elucidate particle interactions underpinning the dewatering behaviour induced by flocculation with polyethylene oxide (PEO), anionic polyacrylamide (PAM A) and their blends. Shear yield stress (τ_y) analysis indicated that polymer mediated particle interactions were markedly amplified upon shear of PEO based pulps. In contrast, PAM A based pulps showed a significant decrease in yield values upon shear. Steady stress measurements analysed using a modified Ellis model indicated subtle differences between the respective linear viscoelastic plateaus of the pulps. Furthermore, modified shear thinning behaviour was evident in PEO based pulps. Estimation of elastic and viscous moduli (G', G'') was made using dynamic stress analysis for comparison with values determined from vane measurements. Despite a noticeable difference in the magnitude of G' between the two methods, similar trends indicating sheared PEO-based pulps to be more elastic than PAM based pulps, were observed. Floc microstructural observations obtained in support of rheological properties indicate that PEO flocculant induces significantly more compact particle aggregation within the clay pulps under shear consistent with the yield stress data, in contrast to PAM A, or indeed unsheared PEO based pulps. Consequentially, sheared PEO based pulps show significantly improved dewatering behaviour. The implications of the results, potential benefits and drawbacks of flocculation with PEO and PAM A are discussed with respect to improvements in current dewatering processes used in the minerals industry.

Keywords : kaolinite, polyethylene oxide, flocculation, elastic modulus, vane rheometry

1. Introduction

The rheology of flocculated mineral tailings has important implications for sustainable mineral processing. It provides tools for assessing thickened tails' consolidation, transportation and geotechnical characteristics, since both time dependent microscopic and macroscopic particle interactions-mediated flow behaviour can be monitored. The measurement of yield (or critical) stress is widely used to characterise pulp rheology and particle interactions, since it has practical (e.g. pumpability and energy requirement) (Sofra and Boger, 2000) and theoretical (e.g. totality of colloidal interaction energy potential), (Scales *et al.*, 1998) ramifications. Pulp shear yield stress is conventionally determined by the vane technique (Nguyen and Boger, 1983). Assessment of compressive yield stress can be determined via centrifugation, or more efficiently through pressure filtration measurements (Usher *et al.*, 2001). Shear and compressive yield stress are strongly correlated, with the magnitude of compressive values 20 – 55 times that of shear yield stress (Zhou *et al.*, 2002; Dustan *et al.*, 2005), however ratios closer to 10 have been reported for clay minerals (Meeten, 1993).

The need for practical and diagnostic assessment of rheological parameters (e.g. yield values, viscosity, elastic and viscous moduli) is apparent when the sustainable treatment and disposal of mineral waste tailings are routinely considered. Consolidation of tails in thickeners usually does not reach static equilibrium by virtue of rapid flow rates and continual rake action. Thus, the dynamic measures of apparent viscosity and shear response of tails under thickener conditions is of relevance and can be assessed through measurement of full flow curves. It is pertinent to note that thickened pulps' high yield stresses limit dewaterability by resisting compaction, however in flocculated systems higher yield stresses incurred may be outweighed by the benefit of improved permeability induced by floc aggregates. Rheological parameters which may be used to predict or control dewatering behaviour either jointly or independently would therefore be of practical value for assessing flocculation and dewatering performance of problematic clay mineral (e.g. kaolinite and smectite) dispersions.

Viscoelastic and yield behaviour can be correlated with the networking size and density of aggregate structures within the pulp. Herrington *et al.* (1993) has linked elevated elastic (G') and viscous (G'') moduli with improved dew-

*Corresponding author: j.addai-mensah@unisa.edu.au

atering performance which were attributed to differences in the kaolinite floc aggregate structure resulting from flocculation with cationic polyacrylamides of different molecular weights. Measurement of G' and G" are typically determined through dynamic (oscillatory) stress analysis, however sample preparation may irreversibly disrupt the particle network. A less disruptive method for estimating the elastic modulus has been demonstrated by Alderman *et al.* (1993) using vane rheometry. Elastic strain is determined from time data which, in combination with torque values prior to yield, can be used to calculate a value for G' (see Section 2.1). This technique has been applied to probe changes in smectite clay pulp particle network structures with and without the presence of high molecular weight xanthan polymer (M'bodj *et al.*, 2004). It was noted that for the same particles under different conditions of coagulation, the same yield stress but significantly different elastic modulus values were obtained, reflecting solid-like differences of the underlying aggregate structure.

Flocculation of clay minerals (e.g. kaolinite and smectite) with conventional high mol. wt. polyacrylamide flocculant (e.g. PAM A) characteristically leads to low sedimented solid loading (solid volume fraction (ϕ) $\approx 0.09 - 0.11$) and shear yield stresses in the range 30 – 70 Pa (Mpofu *et al.*, 2003; McFarlane *et al.*, 2005). Recent investigations have demonstrated that synergistic improvements in sedimentation rates can be achieved by use of dual flocculants (e.g. Weir *et al.*, 2002), however improved consolidation under such conditions is yet to be demonstrated. Significantly increased consolidation of clay based tailings has been achieved by use of non-conventional "shear-sensitive" polyethylene oxide as a flocculant, whereby moderate shear applied to the sedimented flocs of kaolinite and smectite particles resulted in higher solid loadings up to 0.15 – 0.2 v/v (e.g. Mpofu *et al.*, 2003). The shear sensitivity of PEO based flocs has been ascribed to its non-ionic, flexible structure and its strong Lewis base ether oxygen functional group capable of multi-segment adsorption and particle bridging. Flocculation with similar non-ionic polyacrylamide however, has not demonstrated similar behaviour (McFarlane *et al.*, 2005).

In this study, the rheological behaviour of kaolinite dispersions flocculated with high molecular weight non-ionic polyethylene oxide (PEO) and anionic polyacrylamide polyacrylate copolymer (PAM A) of similar molecular weight is characterised and its links to pulp dewaterability established. Dispersions flocculated with a 1:1 blend of the two polymers were also analysed to determine if any synergistic effect was present, impacting on sedimentation and consolidation behaviour. The pulp rheology as determined by vane and controlled stress rheometry was correlated with the dewatering behaviour of the respective dispersions. The dewatering behaviour of the pulps was determined by standard batch settling and pressure filtration tests.

2. Methodology

2.1. Materials and dispersion preparation

Colloidal size kaolinite (K15GM, 99% pure, quartz and mica 1%) particles (Unimin Australia) were used in this work. The particle density and BET surface area were 2.60 $kg \cdot dm^{-3}$ and 27.1 $m^2 \cdot g^{-1}$ respectively with a median particle diameter determined by laser diffraction of less than 5.5 μm. The particle zeta potential determined using an acoustosizer (Colloidal Dynamics) at the experimental pH of 7.5 was –25 mV. The flocculants used were 25 mole% anionically charged polyacrylamide-Na acrylate copolymer (CIBA, Australia) and non-ionic polyethylene oxide (Aldrich) which had nominal molecular weights of 7.5×10^6 Da and 8.0×10^6 Da, respectively. Fresh 0.25 $g \cdot dm^{-3}$ polymer solutions were given a minimum of 16 h mixing at 150 rpm during preparation and were used within 3 days to minimise aging effects. Blended flocculant solution was prepared by mixing equal volumes of the premixed PEO and PAM A solutions for at least 30 min, before addition. A constant level of 250 g $polymer \cdot t^{-1}$ solid was added to the dispersions, representing 1 – 5% of the maximum surface coverage determined by adsorption measurements.

Kaolinite dispersions were prepared at 8 wt% solid by thoroughly mixing a known mass of dry clay in a 5 dm^3 volume of 10^{-3} M KNO_3 electrolyte solution at an agitation rate of 500 rpm for 1 h and allowed to equilibrate quiescently overnight. $MnCl_2$ solution was added to suspensions and pH adjusted to a value of 7.5 30 min prior to flocculation. KOH and HNO_3 (BDH, Australia) were used to adjust pH whenever necessary. The kaolinite dispersions were flocculated in 600 cm^3 beakers at 300 rpm for 15 s. Pulps were then transferred to 500 cm^3 measuring cylinders and left to sediment overnight before rheological measurement. Sheared pulps were prepared by agitating sedimented pulp for 10 min at 100 rpm with a four bladed turbine impeller. The sheared and unsheared pulps can therefore be regarded as representative of the upper and lower shear regimes, respectively encountered in industrial circumstances.

2.2. Vane measurements

Shear yield stress

Vane measurements were controlled with a Haake VT 550 using a 6-blade vane tool. Other experimental parameters are listed in Fig. 1. Shear yield stress (τ_y) was determined in the conventional manner (Nguyen and Boger, 1983), by observing the maximum torque (T_m) and applying the equation

$$T_m = \frac{\pi D^3}{2}\left(\frac{H}{D} + \frac{1}{3}\right)\tau_y \quad (1)$$

where D and H are the vane diameter and height (m), respectively and the units of T_m and τ_y are N·m and Pa, respectively.

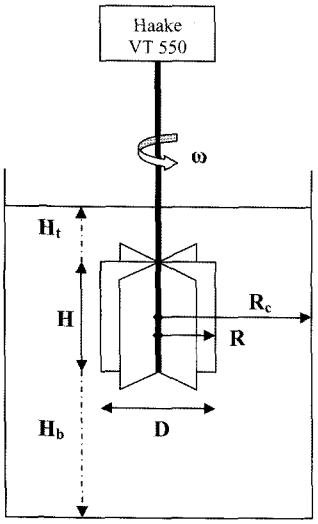

Legend

D = 2R = 22.0 mm
R_c = 24.5 mm
H = 16.0 mm
H_b > 16.0 mm
H_t > 8.0 mm
ω = 0.021 rad·s^{-1}
γ_{app} = ωt/(R_c-R)

Fig. 1. Experimental parameters used for vane measurements.

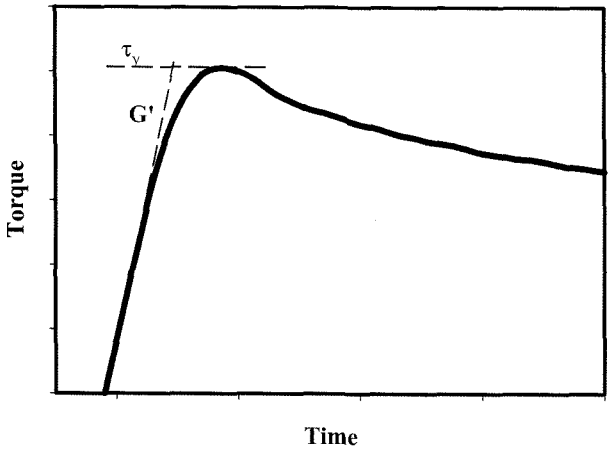

Fig. 2. Generic plot generated by a typical vane measurement showing torque as a function of time from which yield stress, elastic modulus and apparent strains can be calculated.

Elastic modulus

An estimation of the elastic behaviour of the pulp was determined using the method of Alderman *et al.* (1991) whereby the elastic modulus, G' is calculated from the torque-time ratio of the material prior to the maximum torque (Fig. 2), according to the equation

$$G' = \frac{1}{4\pi\omega H}\left(\frac{dT}{dt}\right)\left(\frac{1}{R^2}-\frac{1}{R_c^2}\right) \quad (2)$$

where dT and dt are corresponding torque (N·m) and time (s) increments, respectively and ω (rad·s^{-1}), R (m), R_c (m) and H (m) are dimensional parameters described in Fig. 1. It should be noted that Alderman *et al.* (1991) extrapolated the initial slope before non-Hookean behaviour was established, whereas the data in this study generally did not exhibit Hookean behaviour due to the relatively high minimum rotation rate possible with the Haake VT550. The rheology of sheared pulps was determined after agitating the sedimented pulp with a 4-blade turbine impeller for 10 min and acquiescing overnight. Sediment volumes and measuring cylinder dimensions allowed measurement to be taken *in situ*, thereby requiring minimal disturbance of floc/sediment structure.

2.3. Controlled stress rheometry

Rheological measurements in both static and dynamic modes were conducted using a Rheometrics SR-5000 stress-controlled rheometer with parallel plate sample geometry (40 mm diameter, 2 mm gap). The temperature was maintained at 23 ± 0.1°C with a Peltier element and a thermostatically controlled water bath. For flow curve measurements the applied stress was increased linearly from 10 – 3000 Pa, the deformation determined and viscosity vs. shear stress curves produced. For dynamic measurements the elastic and viscous moduli were determined as a function of applied stress (1 – 3000 Pa) at an oscillation frequency of 1 Hz.

Since samples were significantly disrupted at high stress, fresh samples were used for repeat measurements. Due to the shear sensitive consolidation of PEO flocculated pulps, low solid fraction samples obtained via sedimentation became inhomogenous as a result of shear, *i.e.* solids were concentrated into discrete clumps within a water phase. All pulps were therefore filtered to raise the solid volume fraction to 0.22 – 0.23 by placing 100 cm^3 of pulp between filter paper in a Buchner funnel and placing a 1.2 kg weight onto the cake and allowing 1 h filtration.

Steady shear flow curves of the various kaolinite pulps were characterised using a modified Ellis equation (Roberts and Barnes, 2004):

$$\frac{\eta-\eta_\infty}{\eta_0-\eta_\infty} = \frac{1}{1+\left(\frac{\tau}{\tau_c}\right)^m} \quad (3)$$

where η, η_0, and η_∞ represent the viscosity (Pa·s), low shear viscosity and high shear viscosity respectively, τ and τ_c are the shear stress and critical (yield) stress and m is a power index, m is typically a high number (>5) and can be regarded as indicative of how shear thinning the fluid is.

2.4. Cryogenic scanning electron microscopy

A field emission high resolution scanning electron microscope (SEM) (Philips XL30) was used to examine the smectite structures at various stages along the flocculation process. To avoid internal rearrangement, microgram sized slurry samples were rapidly vitrified in liquid propane at 120 K to arrest supramolecular motion. The vitrified water was then removed by sublimation at 180 K for 2 min. at low pressure to expose clay structures and avoid melting. Samples were then analysed at an accelerating

voltage of 5 kV after sputter coating with Pt to produce a conducting surface.

2.5. Dewatering behaviour

After flocculation of the kaolinite dispersions, settling rates were determined by recording the subsidence of the solid-liquid interface as it receded between 3 and 8 cm below the 500 cm^3 mark. Equilibrium consolidation was taken when no volume change was observed over a 24 h period and was reached in most cases within 24 h after settling commenced. The hindered settling function was determined at high volume fraction using the pressure filtration method described by Usher *et al.* (2001). Dispersions were loaded into cylindrical steel chambers and pressure applied by lowering a piston driven shaft which forced water through a permeable millipore filtration membrane and sintered disk at the base. Pressure and volume changes were continuously recorded and reconciled with permeability data from which hindered settling function as a function of volume fraction was obtained.

3. Results

3.1. Rheology

Full flow curves

Full flow curves obtained for the high solids dispersions flocculated with PEO, PAM A and the polymer blend are compared with unflocculated kaolinite in Fig. 3. The pulps exhibit a non-Newtonian behaviour, with curves comprising a linear viscoelastic plateau up to a critical stress after which a rapid destruction of structure occurs marked by a sharp drop off in viscosity. Initial values of η are most likely underestimated as a result of overestimation of the minimum rotation at low stress (Barnes, 2004). The behaviour of the pulps at high shear rate could not be measured due to sample fragmentation/ejection. As is evident from Fig. 3, the magnitude of both η_0 and τ_c is significantly larger for flocculated samples compared with the unflocculated kaolinite due to polymer bridging forces. Although the drop off from high viscosity is arguably gradual, a four parameter Ellis model (Roberts and Barnes, 2004) provides good correlation with the data.

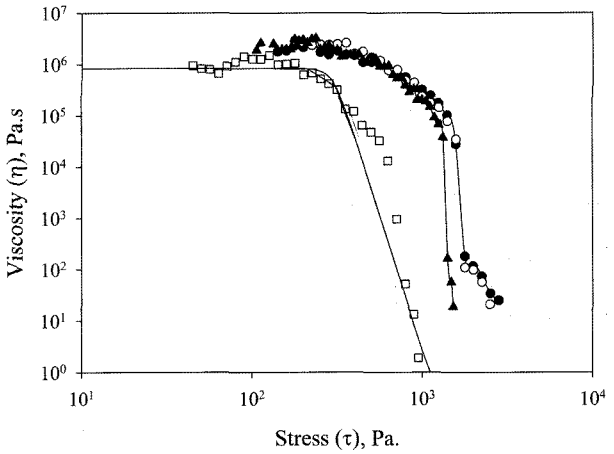

Fig. 3. Full flow curves showing viscosity as a function of applied stress for kaolinite dispersions at 41 wt% solid at pH 7.5 and in 10^{-3} M KNO_3 and 10^{-3} M $MnCl_2$ electrolyte without flocculant (□) and flocculated with PEO (○), PAM A (▲) and 1:1 PAM A/PEO blend (●). The fitted curve obtained from the Ellis model (Eq. 3 in text) is shown for the unflocculated data according to the values of η_0, τ_c and m in Table 3.

The key features of the flow curves are quantified in Table 1. The values obtained for τ_c from steady stress measurements of unflocculated kaolinite dispersions shows close agreement with vane measurements of τ_y (see Table 2 and Fig. 5). The flocculated pulps exhibited decreasing τ_c in the order PEO-blend-PAM A, whereas the η_0 trend decreased in the order blend-PAM A-PEO. These results contrast with the variation in τ_y trends exhibited in vane data (Table 3), which may be the result of different degrees of floc structure modification during filtration and handling. Both flocculated and unflocculated kaolinite pulps exhibit steep declines in viscosity culminating in large values of m (10), indicating that the particle network structure is dramatically rearranged under sufficient stress. This is typical of clay dispersions which show strong shear thinning as a result of alignment of their long axes parallel to the direction of shear (Jogun and Zukoski, 1996).

At low volume fractions (not shown), unflocculated dis-

Table 1. Summary of rheological parameters for flocculated kaolinite determined from plate-plate steady and dynamic stress measurements

Flocculant	Volume fraction	Steady stress			Dynamic stress		
		η_o, Pa·s	τ_c, Pa	m	G', Pa	G'', Pa	τ_c, Pa
No Polymer	0.215	830000 ± 78900	302 ± 30	10.6 ± 1.0	120000	29000	261 ± 25
PEO	0.226	1300000 ± 114000	802 ± 71	10.5 ± 0.92	390000	190000	642 ± 61
Blend	0.219	1600000 ± 159000	707 ± 69	9.8 ± 0.95	310000	160000	511 ± 48
PAM A	0.208	1460000 ± 120000	613 ± 51	11.7 ± 0.88	188000	120000	410 ± 39

Table 2. Scaling law constants fitted to the form $G' = A\phi^B$, $\tau_0 = A\phi^B$ for G' and τ determined by vane and parallel plate rheometry for kaolinite dispersed and in 10^{-3} M KNO_3 electrolyte at pH 4.5

Power law parameters	G', Pa		τ_y and/or τ_c, Pa		
	Vane	Parallel plate (dynamic)	Vane	Parallel plate (dynamic)	Parallel plate (steady)
A, MPa	$2.13 \times 10^{12} \pm 1.0 \times 10^{11}$	$1.02 \times 10^{12} \pm 3 \times 10^{10}$	0.150 ± 0.026	0.555 ± 0.211	0.182 ± 0.060
B	5.0 ± 0.5	5.6 ± 0.3	3.6 ± 0.1	4.5 ± 0.3	3.9 ± 0.2

Table 3. Initial settling rate, consolidation and shear yield stress determined in situ before and after shearing the sedimented pulp

Polymer		No polymer	PAM A	PAM A-PEO blend	PEO
Initial settling rate ($m \cdot h^{-1}$)		0.15 ± 0.002	11.2 ± 1.2	15.4 ± 2.1	22.5 ± 1.5
Pre-shear	Consolidation (wt% solid)	19.1 ± 0.9	16.1 ± 0.8	15.5 ± 0.9	16.1 ± 0.7
	Shear yield stress (Pa)	8.5 ± 0.5	41.8 ± 7.5	25.3 ± 6.3	32.2 ± 6.4
Post-shear	Consolidation (wt% solid)	27.1 ± 0.6	26.7 ± 1.1	27.2 ± 0.6	27.5 ± 1.2
	Shear yield stress (Pa)	34.1 ± 5.5	20.3 ± 5.2	34.4 ± 7.9	59.6 ± 16.7

persions displayed a constant viscosity plateau at high shear rate, however this was not evident for either flocculated or unflocculated dispersions at high volume fraction (Fig. 3). The high stress behaviour of the blend and PEO based pulps show a contrasting behaviour to that of the PAM A flocculated pulp, indicative of differences in the aggregate flow structure. The presence of PEO flocculant induces aggregation upon application of shear (Mpofu *et al.*, 2003), thus further aggregation may be occurring in the high shear rate regime limiting the extent of shear thinning seen for other pulps. Alternatively, the PEO based pulps may comprise more robust aggregates which resist flow alignment and/or floc disaggregation more than the unflocculated kaolinite plates which are free to rotate their long axis into entropically favourable orientations parallel to shear. The shear thinning response of PAM A based flocs at high shear also suggests significant particle alignment, through further disaggregation of the flocs and/or modification of the floc into a more asymmetric shape.

The PEO based pulp high shear viscosity profile may indicate increased flow resistance relative to PAM A based pulps (Fig. 3), thereby requiring greater energy expenditure during pipe transport. Even so, paste like pulps allow improved disposal through tailings stacking rather than impoundment in dams. The treatment of PEO based pulps may therefore require slight modification of a process designed for more shear thinning pulps, such as those based on PAM A. Shorter thickener residence times would allow pumping at lower viscosity and yield stress, after which shear induced by pipe transport may act on the "shear sensitive" PEO based flocs inducing increased consolidation. Further consideration would be required for particular operations to assess whether improved dewatering rates (discussed below) and beneficial disposal efficiencies outweigh the alternative processing requirements.

Shear yield stress

The shear yield stress of sedimented pulps is listed in Table 3 alongside initial settling rates and equilibrium consolidation. Prior to shear, PAM A based pulps exhibited the highest yield stress values which were significantly reduced following shear, due to irreversible rupturing of the floc structure. In contrast, the PEO based pulp, and to a lesser extent the blend based pulps, displayed relatively lower yield stresses which significantly increased following pulp shear, indicating that the particle interactions and networking are increased. Although the sedimented volumes are similar, pulps containing PEO could be consolidated further into a dough-like mass ($\phi = 0.20 - 0.21$) upon gentle squeezing, whilst the PAM A based pulp became less cohesive and uncompactable with similar treatment. Clearly, the presence of PEO induces a different shear response than PAM A based pulps which can be exploited to improve pulp consolidation. Understanding the cause of this behaviour would allow substitution with an analogous flocculant with similar structure and behaviour.

Viscoelastic moduli

A comparison of the elastic modulus values determined by the vane, steady and dynamic stress techniques for a 41 wt% kaolinite pulp as a function of apparent strain is shown in Fig. 4. The range of strains possible with the vane was limited by the minimum rotational speed of the Haake VT550 and the yield strain of the pulps which was generally between 10 and 100% apparent strain. This limitation prevented probing of the Hookean linear viscoelastic region which dynamic measurements exhibit at low strains below 0.1%. It is also apparent that the vane and steady stress data tends to overestimate the elastic modulus with respect to the dynamic measurements. Fitting the vane

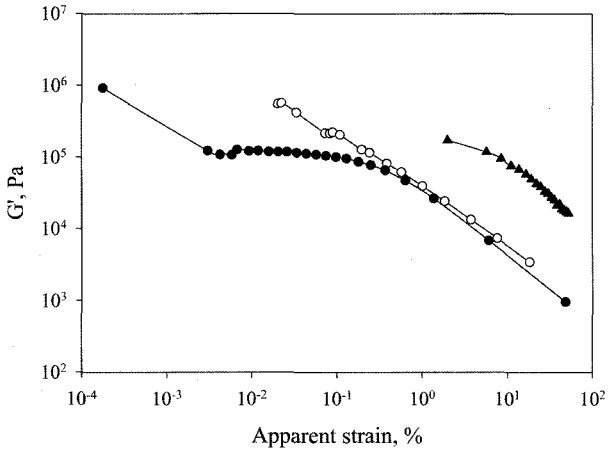

Fig. 4. G' plotted against apparent strain for a 41 wt% kaolinite dispersion at pH 7.5 and in 10^{-3} M KNO_3 and 10^{-3} M $MnCl_2$ electrolyte as measured by dynamic stress (●), steady stress (○) and vane (▲) rheometry.

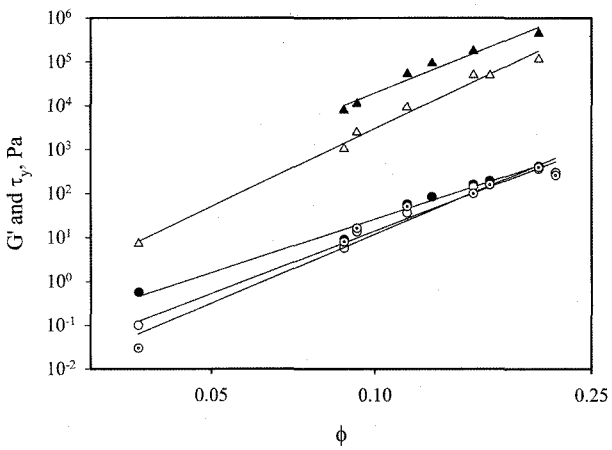

Fig. 5. Shear yield stress and elastic modulus of kaolinite dispersions as a function of volume fraction comparing vane and dynamic measurements showing trendlines fitted according to $G' = A\phi^B$, $\tau_y = A\phi^B$.

data to the power law $G' = A\phi^B$ gives values for A and B of $2.1 \times 10^{12} \pm 1 \times 10^{11}$ MPa and 5.0 ± 0.5, respectively (see Fig. 5, Table 2). Values determined from dynamic measurements for A and B of $1.0 \times 10^{21} \pm 3 \times 10^{10}$ MPa and 5.6 ± 0.3, respectively indicate that similar scaling behaviour is displayed between the two methods. Thus, in spite of differences in magnitude, the systematic trends indicate qualitative agreement between the two techniques, justifying the use of vane data to estimate the elastic modulus trends in flocculated pulps.

The elastic modulus as a function of strain determined by the vane for flocculated pulps measured in situ after sedimentation is displayed in Fig. 6A. The influence of polymer bridging is seen in the increased G' values exhibited relative to the unflocculated kaolinite plot. Prior to shear

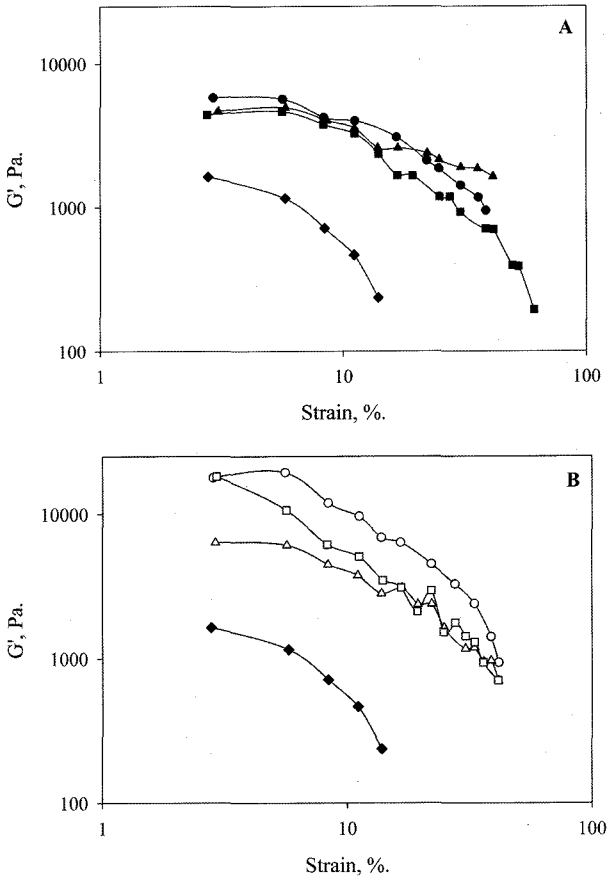

Fig. 6. G' vs. apparent strain for 26 wt% kaolinite dispersion at pH 7.5 and in 10^{-3} M KNO_3 and 10^{-3} M $MnCl_2$ electrolyte without flocculant (◆) and flocculated with PEO (●), PAM A (▲) and 1:1 PAM A/PEO blend (■), with (A) and without (B) pulp shear.

however, G' values follow similar trends irrespective of the flocculant, in contrast to the corresponding yield stress data (Table 3). Following pulp shear (Fig. 6B), increased elastic modulus values were exhibited by the PEO based pulps suggesting, as did τ_y data, that increased particle interactions are induced by shear. The elastic modulus of PAM A based pulps was unchanged, whereas the yield stress data decreased as a result of shear treatment. It is of interest to compare the G' trends exhibited by pulps with similar yield stresses, in this case the PEO based pulp after shear and the PAM A based pulp prior to shear. The PEO based pulps are markedly more elastic than the respective PAM A based pulp, suggesting differences in the flocs/pulp structure are present which are not reflected by the yield stress.

The elastic moduli of kaolinite suspensions at higher solid volume fraction (0.2 – 0.21), were determined using dynamic stress (Fig. 7). The G' and G'' values in the linear viscoelastic region display magnitudes which decrease in the order PEO-blend-PAM A-no flocculant, as did the τ_y values (Table 1). Although these trends are concurrent with

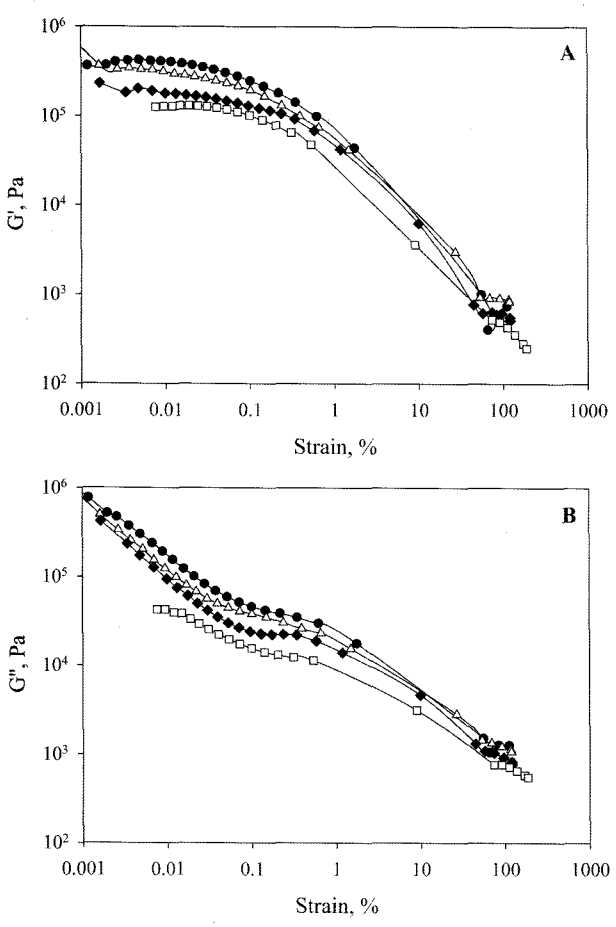

Fig. 7. Elastic moduli G' (A) and G'' (B) plotted against apparent strain from dynamic stress of kaolinite dispersions at 26 wt% solid at pH 7.5 and in 10^{-3} M KNO_3 and 10^{-3} M $MnCl_2$ electrolyte without flocculant (◆) and sheared pulps flocculated with PEO (●), PAM A (▲) and 1:1 PAM A/PEO blend (■).

a slight difference in solid content, the scaling behaviour is insufficient to account for the difference in magnitude. Somewhat unusually, the G'' values at strains below 0.1% (Fig. 7B) display a monotonically increasing upward trend in flocculated pulps. SEM micrographs of the flocculated kaolinite pulps in Fig. 8 indicate that the flocculated clay microstructure comprises an extensive cell or honeycomb structure. Thus, at very small strains, the particles retain strong colloidal contacts that resist deformation, constrained by the pre-existing structure. At intermediate strains prior to the critical point, an equilibrium between structural breakdown and reconstruction takes place, resulting in the linear G'' region. After the critical point is reached, the particles or flocs behave predominantly as individual flow units. Optimum dewatering is envisaged as occurring when the viscous modulus is minimum but preceding disaggregation of the solid phase, that is coinciding with the linear G'' region prior to rapid structural breakdown of the particle/floc network.

3.2. Floc microstructure

SEM micrographs of unflocculated and flocculated kaolinite displayed in Fig. 8 provide a qualitative assessment of kaolinite aggregate structures. Unflocculated kaolinite particles (Fig. 8A) appear to comprise 2 – 6 μm aggregates with either weak or non-existent interactions between aggregates. It is unclear whether the aggregates represent the primary colloidal particles, or the coagulated particle structure, however in either case they are most likely the basic unit of polymeric floc construction. The microstructure of undisturbed pulp flocculated with PEO (Fig. 8B) indicates that aggregates are clustered into a partially interconnected porous network with pores 6 – 10 μm in diameter, reminiscent of honeycomb structures seen in images of flocculated smectite particles elsewhere (McFarlane *et al.*, 2005). After shear, the microstructure of PEO-based aggregates (Fig. 8D) display greater particle interactions, forming a less porous and weakly interconnected particle network.

The microstructure of unsheared pulp flocculated with PAM A (not shown) closely resembled that of the unsheared PEO based flocs (Fig. 8B). However in contrast to the sheared PEO based pulp, the kaolinite microstructure of sheared PAM A based pulp (Fig. 8C) exhibits only slight inter-aggregate contact whilst retaining vestiges of the more extensive network displayed in unsheared flocculated pulp. Shear therefore appears to disrupt the polymer mediated floc network, without completely re-establishing the dispersed structure exhibited by unflocculated dispersions (Fig. 8A).

3.3. Dewatering behaviour

The subsidence rates of flocculated kaolinite dispersions before and after shear are shown in Fig. 9A and 9B respectively. Prior to shear, the flocculated dispersions display marginal differences in settling rate but a significant increase in comparison to the unflocculated dispersion. Following shear the subsidence rates increase as the PEO proportion increases. While the post shear data trends closely follow the τ_y and G' trends (Table 3 and Fig. 5), only the G' data can be correlated with the dewatering trends. For example, prior to shear PAM A based pulps exhibit higher yield stresses than those of PEO whereas the G' data are similar to one another, as are the sedimentation curves. The yield stress of the PEO based pulp following shear is similar to that of the PAM A based pulp before shear, whereas the G' of the sheared PEO based pulp is significantly higher than that of the unsheared PAM A based pulp, again demonstrating the correspondence between G' and subsidence rate trends.

The dewatering behaviour at high volume fraction is shown in Table 4. Flocculation significantly increased the volume fraction at which the selected dewatering rate could be attained from 0.09 to 0.23. Thus, for a similar pore volume, the flocculated kaolinite dispersion comprised denser

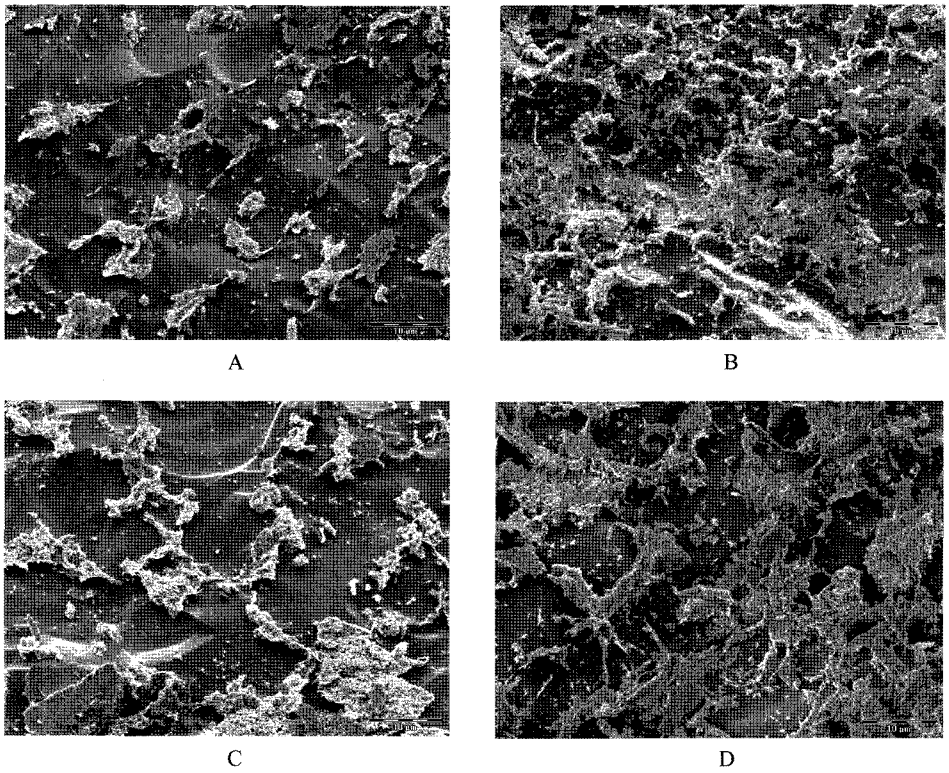

Fig. 8. SEM micrographs of cryogenically immobilised kaolinite dispersions at ≈41 wt% solid at pH 7.5 and in 10^{-3} M KNO_3 and 10^{-3} M $MnCl_2$ electrolyte without flocculant (A) and flocculated with PEO without shear (B), PAM A following shear (C) and PEO following shear (D).

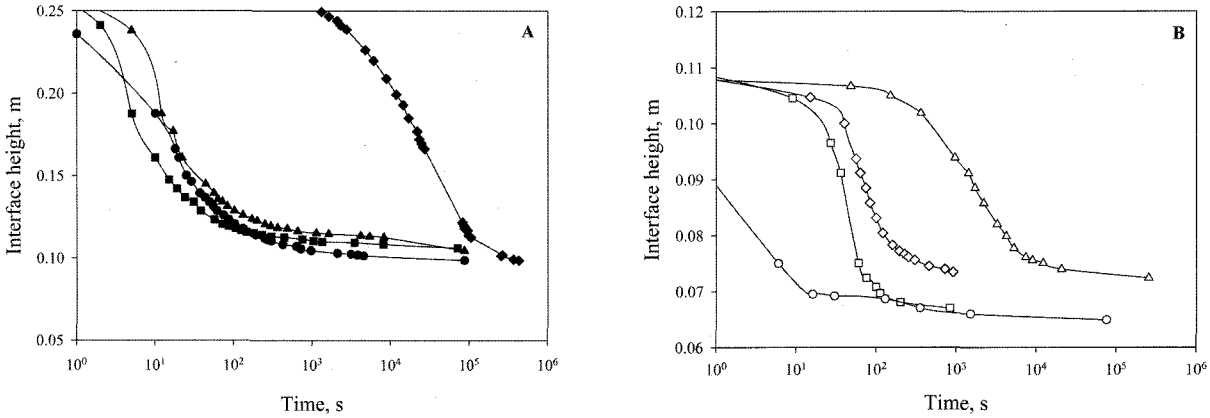

Fig. 9. (A) Subsidence of kaolinite dispersions at 8 wt% solid at pH 7.5 and in 10^{-3} M KNO_3 and 10^{-3} M $MnCl_2$ electrolyte prior to shear as a function of time. Symbols denote PEO (●), PAM A (▲) and 1:1 PAM A/PEO blend (■) and no flocculant (◆) and (B) Subsidence of kaolinite dispersions at 16 wt% solid at pH 7.5 and in 10^{-3} M KNO_3 and 10^{-3} M $MnCl_2$ electrolyte following shear as a function of time. Symbols denote PEO (○), PAM A (△) and 1:1 PAM A/PEO blend (□) and 3:1 PAM A/PEO blend (◇).

aggregates than the unflocculated dispersion, which also correlates with the SEM micrographs (Fig. 8). Following shear, the volume fraction of the PAM A based pulps decreased whereas that of the PEO based pulps increased, reflecting diminished and enhanced aggregate density, respectively. Yield stress data (Table 3 and Fig. 3) indicates that flocculation imparts a greater resistance to yield, and on this basis should decrease the capacity for improved pulp dewatering. Flocculation must therefore impart the pulp with improvements in permeability which offset the effect of increased yield stress. The possibility of high yield stress being an indicator of improved dewaterability is invalidated by the difference in behaviour between the unsheared PAM A based pulps and the sheared PEO based pulps which both

Table 4. Solids volume fraction achieved by kaolinite dispersions at a hindered settling function data of $R(\phi)\ 3 \times 10^{11}$ $Kg \cdot s^{-1} \cdot m^{-3}$

Flocculant	Volume fraction (at $R(\phi) \approx 3 \times 10^{11}$ $Kg \cdot s^{-1} \cdot m^{-3}$)	
	Pre shear	Post shear
None	0.09	-
PAM A	0.233	0.192
PAM A/PEO blend	-	0.285
PEO	0.235	0.392

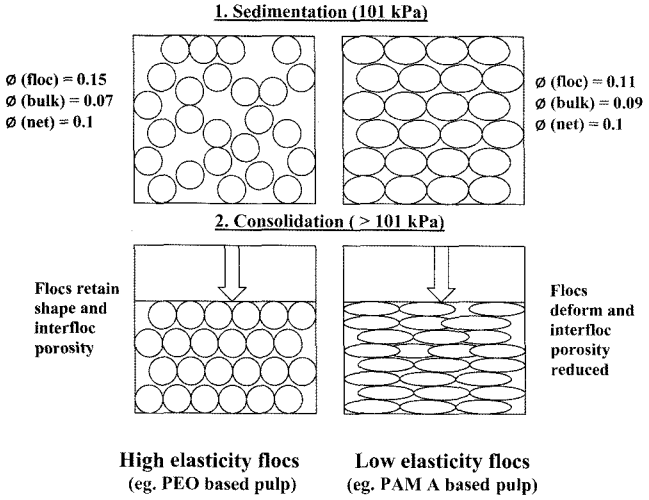

Fig. 10. Schematic showing pulp structure differences resulting from flocs of high elasticity and volume fraction (left) in contrast to those of low elasticity and solid fraction (left). During sedimentation (top) an equivalent bulk solid fraction corresponds to higher porosity and dewatering rate in high density flocs. Application of further pressure (bottom) induces greater deformation of less elastic flocs resulting in diminished pore space relative to more elastic flocs at the same total solid fraction.

exhibited similar, relatively high yield stresses.

3.4. Discussion

An explanatory summary of the rheological, microstructural and dewatering observations is depicted in Fig. 10. Densely aggregated flocs are desirable for improved dewatering, since they provide greater pore space through which water can escape, thereby increasing settling and consolidation (Farrow *et al.*, 2000). Under a compressive load, denser flocs are more capable of resisting flattening, thereby retaining more open pore structures relative to less dense, easily deformed flocs (Besra *et al.*, 2002). Thus, the flocs which exhibit higher G' values indirectly indicate more densely aggregated flocs and thus more open interfloc pore space, as well as being a direct indication of greater resistance to deformation. Since it is likely that inter floc water is significantly more mobile than intrafloc water, it is reasonable to expect that the floc density influences the permeability of the system significantly at "low" volume fractions. At some higher volume fraction, the internal floc characteristics will become more significant in the overall dewaterability of the system at which point, the elastic, dense flocs may inhibit dewatering more than the deformable lower density flocs. For practical purposes however, this point is likely to exceed the volume fractions obtained in thickener operations, and therefore only of possible relevance to extended dewatering times typical in tailings impoundments.

The respective pulps exhibit only subtle differences in their steady shear behaviour in spite of significant dewatering behaviour and microstructural differences. This suggests that the macroscopic network strength and flow behaviour are largely influenced by the overall solid volume fraction rather than the underlying differences in particle distribution and spatial arrangement (i.e. porosity). Since the sheared PEO based pulp is capable of much more rapid dewatering than the sheared PAM A based pulp, a similar thickener residence time would likely result in significantly increased underflow rheology, and possibly require some adjustment to regular procedure.

Examination of data of different clay mineral surfaces indicates similar correlations between G' and dewatering behaviour, however the absolute magnitudes do not. Smectite pulps for example, exhibit poorer dewatering behaviour and higher yield stresses and elastic moduli with respect to the kaolinite pulps shown here. They do however, display similar polymer related trends in their G'-strain behaviour. The yield value and viscoelasticity differences may arise from the fundamental particle properties such as specific interfacial chemistry and physical attributes such as aspect ratio or hydrophobicity.

The blending of PAM A and PEO flocculants displayed intermediate properties of the individual rheological and dewatering behaviour. Whilst possible synergistic effects were not observed, the shear consolidation response of PEO flocculated pulps was reduced but not entirely eliminated in the presence of PAM A.

4. Conclusions

The rheological behaviour of flocculated kaolinite dispersions has been investigated by vane, steady and dynamic stress rheometry, and compared with the microstructure and dewatering behaviour exhibited at low and moderate volume fractions. Full flow curves exhibit viscosity, critical stress and shear thinning characteristics which are predominantly controlled by the volume fraction displaying subtle differences resulting from flocculant selection. The presence of PEO modified the high shear behaviour of the kaolinite pulp in comparison to the pres-

ence of PAM A or no flocculant.

Estimation of the elastic modulus indicated good agreement between the scaling exponent determined using dynamic measurement and the vane. Vane measurements were then used to assess differences between the sedimented pulps resulting from settling tests. Prior to any disturbance, similar magnitudes of G' were exhibited by PEO and PAM A based pulps which were much larger than the values exhibited for unflocculated kaolinite pulp. Following a period of shear, the magnitude of G' was dramatically increased in PEO based pulps, whereas that of PAM A pulps was unchanged. Microstructural analysis indicates that the trends in G' magnitude correspond with increased density of kaolinite particle within flocs. The dewatering characteristics of the pulps also showed correspondence with the G' data, whereby increased G' was indicative of more rapid dewatering of the pulp. Thus flocculation with PEO enables densification of the aggregate structures which allows greater pore volume through which water can be removed. Using G' as calculated from vane measurements may therefore provide a useful diagnostic tool for predicting the relative effectiveness of polymeric additives on the dewatering process.

Acknowledgements

The authors gratefully acknowledge AMIRA International and P523A sponsors: Rio Tinto, Anglo Platinum and Newmont and the ARC for financial support. AM is indebted to Shane Usher and Yasushi Saiki for advice and discussion and Peter Self for tireless assistance obtaining SEM images.

List of Symbols used

- τ : shear stress
- τ_y : shear yield stress determined by vane measurement
- τ_c : critical yield stress determined by dynamic or steady parallel plate measurement
- ϕ : volume fraction of solids such that $V_{solid} : V_{solid} + V_{liquid}$
- G' : elastic modulus
- G'' : viscous modulus
- η : viscosity
- η_0 : zero shear viscosity determined in linear viscoelastic region
- η_∞ : infinite shear viscosity, approximated to minimum measured viscosity in many cases.
- γ : strain
- ω : angular velocity
- m : power law index for Eq. 3
- T_m : maximum torque determined during vane measurement

References

Alderman, N. J., G. H. Meeten and J. D. Sherwood, 1991, Vane rheometry of bentonite gels, *Journal of Non-Newtonian Fluid Mechanics* **39**(3), 291-310.

Barnes, H. A. and D. Bell, 2003, Controlled-stress rotational rheometry: An historical review, *Korea-Australia Rheology Journal* **15**(4), 187-196.

Besra, L., D. K. Sengupta, S.K. Roy and P. Ay, 2002, Flocculation and dewatering of kaolin suspensions in the presence of polyacrylamide and surfactants, *International Journal of Mineral Processing* **66**, 203-232.

Farrow, J. B., R. R. M. Johnston, K. Simic and J.D. Swift, 2000, Consolidation and aggregate densification during gravity thickening, *Chemical Engineering Journal* **80**(1-3), 141-148.

Herrington, T. M., B.R. Midmore and J.C. Watts, 1993, Flocculation of kaolin suspensions by polyelectrolytes, Colloid-polymer interactions: particulate, amphiphilic and biological surfaces. Penger Tong and Paul L. Dubin (Eds), ACS, Washington D.C.

Jogun, S. and C.F. Zukoski, 1996, Rheology of dense suspensions of platelike particles, *Journal of Rheology* **40**, 1211-1232.

M'bodj, O., N. Kbir Ariguib, M. Trabselsi Ayadi and A. Magnin, 2004, Plastic and elastic properties of the systems interstratified clay-water-electrolyte-xanthan, *Journal of Colloid and Interface Science* **273**, 675-684.

McFarlane, A. J., J. Addai-Mensah and K. Bremmell, 2005, Improved dewatering behaviour of clay dispersions via optimised interfacial chemistry and particle interactions, *Journal of Colloid and Interface Science* **294**, 116-127.

Meeten, G.H., 1993, Shear and compressive yield in the filtration of a bentonite suspension, Colloids and Surfaces A: Physicochemical and Engineering Aspects.

Mpofu, P., J. Addai-Mensah and J. Ralston, 2003, Investigation of the effect of polymer structure type on flocculation, rheology and dewatering behaviour of kaolinite dispersions, *International Journal of Mineral Processing* **71**, 247-268.

Nguyen, Q. D. and D. V. Boger, 1983, Yield stress measurement for concentrated suspensions, *Journal of Rheology* **27**, 321-349.

Roberts, G. P., H. A. Barnes and P. Carew, 2001, Modelling the flow behaviour of very shear-thinning liquids, *Chemical Engineering Science* **56**(19), 5617-5623.

Scales, P. J., S. B. Johnson, T. W. Healy and P.C. Kapur, 1998, Shear yield stress of partially flocculated colloidal suspensions, *AIChE Journal* **44**, 538-544.

Sofra, F. and D. V. Boger, 2002, Environmental rheology for waste minimisation in the minerals industry, *Chemical Engineering Journal* **86**(3), 319-330.

Usher, S. P., R. G. de Krester and P.J. Scales, 2001, Validation of a new filtration technique for dewaterability characterization, *AIChE Journal* **47**(7), 1561-1570.

Zhou, Z., P. J. Scales and D. V. Boger, 2001, Chemical and physical control of the rheology of concentrated metal oxide suspensions, *Chemical Engineering Science* **56**(9), 2901-2920.